2018

Versatile soliton emission from a WS2 mode-locked fiber laser

Bo Guo

Shi Li

Ya-xian Fan

See next page for additional authors

Funder: Fundamental Research Funds for the Central Universities; National Natural Science Foundation; Key Program for International S&T Cooperation Projects of China; Key Program for Natural Science Foundation of Heilongjiang Province of China; Harbin Engineering University

Authors
Bo Guo, Shi Li, Ya-xian Fan, and Pengfei Wang

Optics Communications 406 (2018) 66–71

Contents lists available at ScienceDirect

Optics Communications

journal homepage: www.elsevier.com/locate/optcom

Versatile soliton emission from a WS_2 mode-locked fiber laser

Bo Guo [a,*], Shi Li [a], Ya-xian Fan [a], Pengfei Wang [a,b]

[a] Key Lab of In-Fiber Integrated Optics, Ministry Education of China, Harbin Engineering University, Harbin 150001, China
[b] Photonics Research Centre, Dublin Institute of Technology, Kevin Street, Dublin 8, Ireland

ARTICLE INFO

Keywords:
Mode-locked fiberlaser
Soliton
Saturable absorber
Two-dimensional materials
WS_2

ABSTRACT

Recently, few-layer tungsten disulfide (WS_2), as a shining 2D material, has been discovered to possess both the saturable absorption ability and large nonlinear refractive index. Here, we demonstrate versatile soliton pulses in a passively mode-locked fiber laser with a WS_2-deposited microfiber. The few-layer WS_2 is prepared by the liquid-phase exfoliation method and transferred onto a microfiber by the optical deposition method. Study found, the WS_2-deposited microfiber can operate simultaneously as a mode-locker and a high-nonlinear device. In experiment, by further inserting the WS_2 device into the fiber laser, besides the dual-wavelength soliton, noise-like soliton pulse, conventional soliton and its harmonic form are obtained by properly adjusting the pump strength and the polarization states. For the dual-wavelength soliton pulses and noise-like pulse, the maximum output power of 14.2 mW and pulse energy of 4.74 nJ is obtained, respectively. In addition, we also achieve the maximum harmonic number (135) of conventional soliton, corresponding to a repetition rate of ~497.5 MHz. Our study shows clearly that WS_2-deposited microfiber can be as a high-nonlinear photonic device for studying a plenty of nonlinear soliton phenomena.

1. Introduction

Since firstly demonstrated in 1986, mode-locked fiber lasers have gained great attentions owing to their potential applications in the fields of micromachine, sensing, optical metrology and biomedicine [1]. An important goal of the mode-locked fiber lasers is to achieve soliton operation. It provides an excellent framework for understanding complex nonlinear phenomena and stimulates novel cavity designs. Reciprocally, the mode-locked fiber laser serves as an ideal platform for testing the concept of solitons and revealing their versatile dynamics. By properly selecting the laser cavity parameters, various kinds of soliton pulses including conventional soliton, similariton [2], dissipative soliton [3], and noise-like soliton pulse [4], have been demonstrated in the lasers. Among them, the highly cavity nonlinearity plays an important role in the formation and evolution of soliton pulses [5–14]. Generally, to obtain high nonlinearity in the cavity it can be achieved by improving the pump power or inserting a length of highly nonlinear fiber. For example, Vazquez-Zuniga et al. obtained the noise-like pulses in a passively mode-locked fiber laser with a 12-m highly nonlinear fiber [15]. However, it greatly increases the cost and difficulty. Thus, it is urgent to seek the highly nonlinear photonic device.

Recently, 2D nanomaterials, namely graphene [16–20], topological insulators (TIs) [21–23], transition metal dichalcogenides (TMDCs) [24–28], and black phosphorus (BPs) [29,30], have gained great attention in physics, chemistry and material fields due to their potential applications. Among them, few-layer WS_2, as one of TMDCs, has been widely used for constructing mode-locked [31–39] or Q-switched [40–45] fiber lasers at the wavelength range of 0.6–2 μm due to their broadband saturable absorption and pulse-shaping ability. Interestingly, besides saturable absorption, few-layer WS_2 exhibits a huge Kerr refractive index with a value of 10^{-11} m^2/W due to the comprehensive contribution of both bound-electronic and free-carrier nonlinearities [38], which is one order of magnitude greater than that of graphene and favorable for versatile soliton pulse generation but not fully explored yet. Moreover, few study concerns the dual-property of the WS_2 device, namely, saturable absorption and high-nonlinearity, which relates to the real part and imaginary part of third-order nonlinear refractive index of few-layer WS_2, respectively. Thus, a question arises naturally: is it possible to generate the versatile soliton pulses in a fiber laser with few-layer WS_2? The exploration of this question will help us to understand the nonlinear optical property of few-layer WS_2 and design the novel lasers.

Here, we experimentally demonstrated the versatile soliton pulses in a passively mode-locked fiber laser with a WS_2-based microfiber. The WS_2 device can be as both a mode-locker and a high-nonlinear medium simultaneously. By utilizing the dual optical properties of

* Corresponding author.
E-mail address: guobo512@163.com (B. Guo).

http://dx.doi.org/10.1016/j.optcom.2017.05.042
Received 1 April 2017; Received in revised form 6 May 2017; Accepted 16 May 2017
Available online 7 June 2017
0030-4018/

the WS_2 photonic device, dual-wavelength soliton, noise-like pulse, conventional soliton and its harmonic form are obtained by properly adjusting the pump strength and the polarization state in the cavity. This work provides an example of the WS_2-deposited microfiber could both be as both a mode-locker and an excellent high-nonlinear medium for versatile soliton formation.

2. Preparation, characterization of microfiber-based WS_2 device

The high-quality WS_2 nanosheets as-used in this experiment were prepared through the liquid-phase exfoliation method [31]. The concentration of WS_2 nanosheets in the solvent is about 0.1 mg/ml, as shown in the inset of Fig. 1(a). Firstly, we transfer the WS_2 solution onto a sheet of quartz glass and dry at the room temperature so as to character its property. Then, the crystalline structure of the WS_2 material was characterized by using Raman system at 514 nm. Fig. 1(a) shows the Raman spectrum of the WS_2 nanosheets in the range of 280–480 cm^{-1}. It can be clearly seen that there are two typical Raman peaks located at ~352.6 and ~418.1 cm^{-1}, corresponding to in-plane vibrational mode E^1_{2g} and out-plane vibrational mode A_{1g} of S–W–S lattice vibration, respectively. Next, we characterized its morphological properties with a scanning electron microscopy (SEM) and atomic force microscope (AFM), as shown in Fig. 1(b) and (c), respectively, which reveal that the WS_2 material exhibits sheet-like structure with wide distribution.

To realize the all-fiber laser and further enhance the nonlinearity in the laser cavity, we will transfer the few-layer WS_2 onto the waist of microfiber with the optical deposition method, forming a microfiber-based WS_2 device. The microfiber with the waist diameter of ~20 μm, was prepared by fused taper method, as shown in the inset of Fig. 2. The saturable absorption property of the WS_2 device plays an important role for the generation of soliton pulse. Seen clearly from the Fig. 2, its saturation intensity, modulation depth and nonsaturation loss is about 42.6 MW/cm^2, 1% and 6.2%, respectively, which measured by power-dependent transmission scheme [38]. The as-used pump source is a mode-locked fiber laser. Its central wavelength, pulse width and repetition rate are 1550 nm, 300 fs and 15 MHz. Additionally, we provided the total cavity loss of the WS_2 device is about 3 dB, which was measured with an optical power meter.

3. Experimental setup

The experimental scheme of the mode-locked fiber laser is shown in Fig. 3. The pump source is a fiber-pigtailed 980 nm laser diode (980-420-B-FA, LD) and transferred the energy to a piece of ~5 m Erbium-doped fiber (Core active L-900, EDF) with dispersion parameter of ~−16.3 ps/(km nm) via a 980/1550 wavelength-division multiplexer (WDM). The single mode fiber (SMF) varies 50 m and 90 m and its dispersion parameter is ~18 ps/(km nm). A 10% optical coupler (OC) is used to extract the laser output. A polarization-independent isolator (ISO) is used for unidirectional operation of the fiber laser and a polarization controller (PC) is used to adjust the polarization state in the cavity, respectively. To enhance the nonlinear effect in the cavity, the microfiber-based WS_2 device was spliced right after the PC. The pulse information and laser power obtained is measured by an optical spectrum analyzer (YOKOGAWA, AQ-6370C) with the resolution of 0.01 nm, a 1 GHz mixed oscilloscope (Tektronix MDO4054-6, 5 GHz/s) combined with a high-speed photo-detector (Thorlabs PDA, 10 GHz) and an optical power meter, respectively.

4. Results and discussions

Before carrying out this experiment, we firstly measured the operation characteristics of the laser without incorporating the WS_2 device. By adjusting the pump power from 0 to 420 mW and polarization states from 0° to 180°, there is no mode-locking generation, which excludes the possibility of NPR and the Fabry–Perot effect in the cavity.

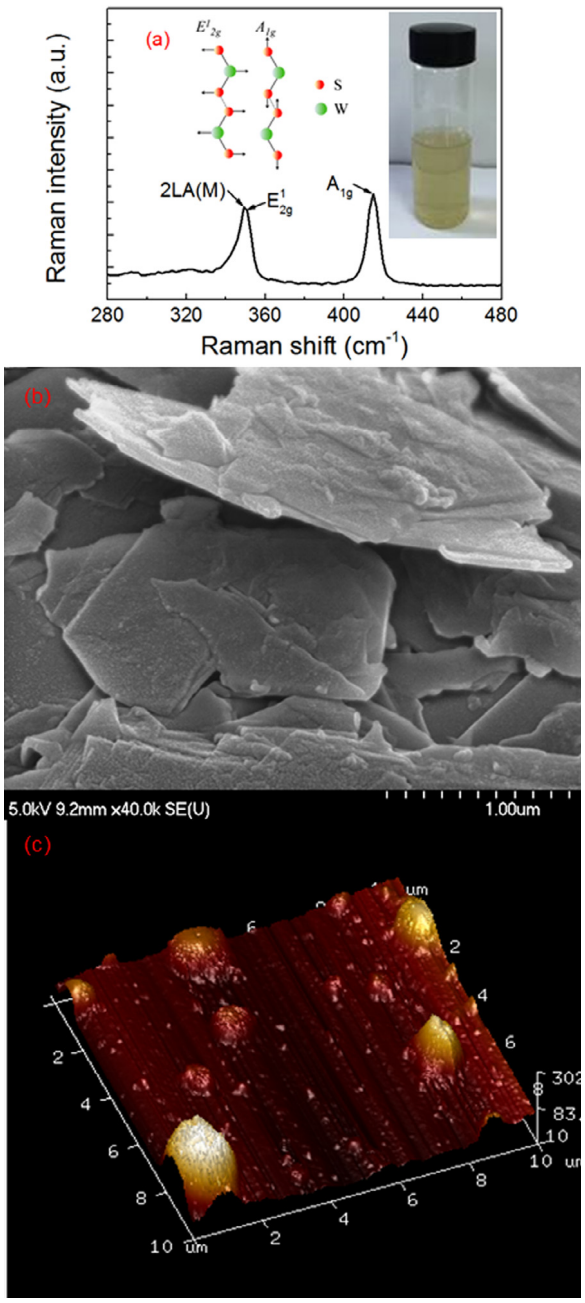

Fig. 1. Typical characteristics of the WS_2 nanosheets: (a) the Raman spectrum, inset: the photograph of WS_2 sample, (b) the SEM, and (c) the AFM.

Then, we inserted the WS_2-deposited microfiber into the laser cavity when the length of SMF is ~50 m, corresponding to the cavity dispersion parameter value of −1.09 ps^2. Initially, continue wave operation started at ~18 mW and the dual-wavelength mode-locking operation occurred at ~72 mW. Thereafter, the dual-wavelength soliton state can be achieved by properly adjusting the polarization states when the pump power continuously increased from 72 to 210 mW. Notably, the dual-wavelength soliton is developed from two CWs lasing, which indicates the existence of the cavity birefringence filter [46]. Normally, the filtering effect can be ignored in the weakly birefringent fiber lasers where the cavity birefringence induced artificial birefringence filter has a large bandwidth. However, the situation may be changed in our experiment. As mentioned above, if no WS_2 device exists, it will be no dual-wavelength lasing appears whatever adjust the pump power and polarization states in a wide range. Thus, the microfiber-based WS_2

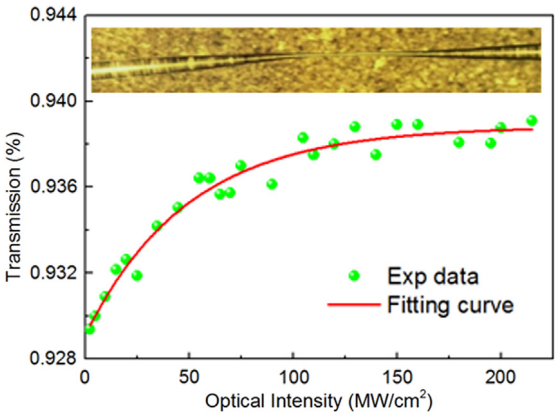

Fig. 2. The nonlinear saturable absorption curve of the microfiber-based WS_2 device.

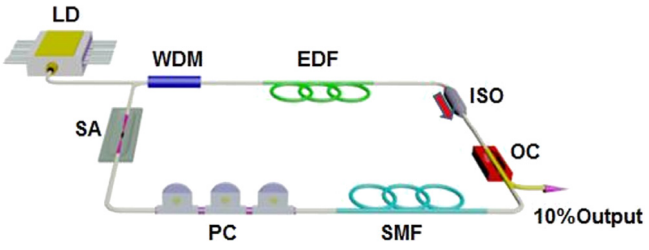

Fig. 3. Experimental setup.

device should play a key role for enhancing the filtering effect in the cavity.

Fig. 4 summarizes the typical dual-wavelength soliton operation under the pump power of ~120 mW in our proposed fiber laser. Fig. 4(a) is the spectrum on a logarithmic scale. It can be seen that, the whole spectrum contains two separated parts with a central wavelength of 1568.55 nm (λ_1) and 1569 nm (λ_2), respectively, which indicates the existence of two different pulses. Clearly, there is a pair of symmetric Kelly sideband appears on the each separated spectrum, which is a typical characteristic of soliton pulse in the lasers [3]. For the dual-wavelength soliton pulses, its wavelength separation and 3-dB spectral bandwidth per-lasing wavelength is ~0.45 nm and ~0.27 nm, respectively. Fig. 4(b) illustrates the pulse trains of the dual-wavelength soliton recorded by an oscilloscope with a time span of 12 μs. There are two pulses equidistantly distributed with a fixed separation of ~467.4 ns in one cavity period, corresponding to a fundamental cavity frequency of ~2.14 MHz. To further confirm that the soliton pulses appeared in our cavity are the dual-wavelength pulses but not multiple pulses induced by energy quantization effect [47], it needs to measure the pulse profile of the dual-wavelength soliton. In experiment, one wavelength (λ_2) was filtered out by using a bandpass filter. Its autocorrelation trace was measured by using a commercial autocorrelator with large scanning range, as illustrated in the inset of Fig. 4(b). Clearly, there was only one pulse appeared. If a $sech^2$ profile is assumed for fitting, the pulse duration is about 11 ps. Thus, the time–bandwidth product (TBP) is ~0.33, which is close to the theoretical limit value (0.315) and indicates that the soliton pulse was slightly chirped. In order to examine the long-term stability of the mode-locked lasers, we continuously monitor the output spectra of the mode-locked pulse for 16 h. Fig. 4(c) shows the evolution of the optical spectra of the dual-wavelength soliton pulses, indicating the stability of the mode-locked fiber laser. Furthermore, we also measured the output power characteristics of the laser, as shown in Fig. 4(d). It can be seen that, the laser exhibits a slope efficiency of ~3.65%. When

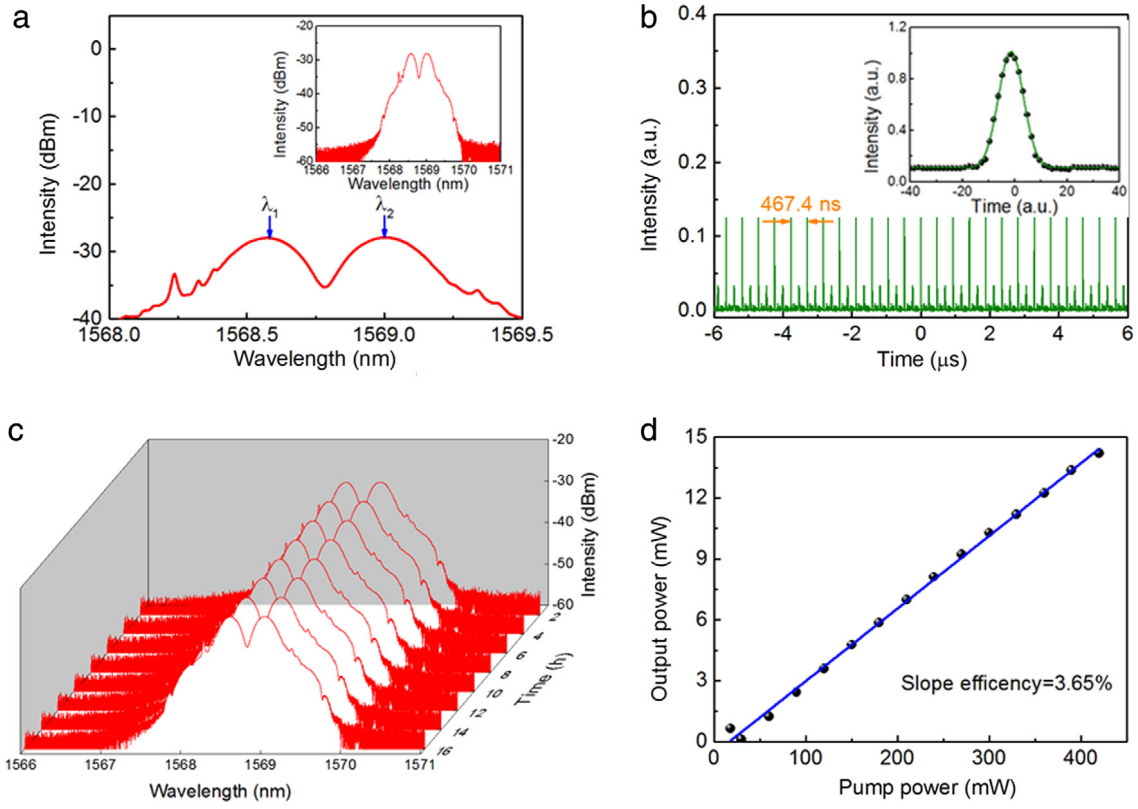

Fig. 4. Dual-wavelength soliton operation with a SMF length of ~50 m and a pump power of ~120 mW: (a) optical spectrum, (b) its corresponding oscilloscope trace (inset: the autocorrelation trace), (c) long-term optical spectra measured at a 2-h interval over 16 h, and (d) the output power versus the pump power.

Table 1
Summary of the dual-wavelength soliton lasers near 1550 nm.

Mode-locked mechanism	Central Wavelength/nm	Wavelength spacing/nm	Repetition frequency/MHz	Pulse duration/ps	Output power/mW	Pulse energy/nJ	Reference
NALM	1563, 1567.5	4.5	–	–	–	–	[5]
NPR	1560.7, 1601.9	41.2	–	28	–	–	[6]
NPR	1532, 1555	23	–	–	–	–	[7]
NPR	1562, 1605	43	–	–	–	–	[8]
NPR	153, 1555	25	–	–	–	–	[9]
NPR	1533, 1546	13	–	–	–	–	[10]
CNT	1532, 1557	25	–	–	0.248	–	[11]
CNT	1549.5, 1559.5	10	–	–	–	–	[12]
CNT	1531, 1557	26	–	–	–	–	[13]
h-BN	1531.5, 1557.5	26	2.21	1.3	7.2	3.4	[14]
Bi_2Te_3	1557.4, 1559.4	2	388	1.3	–	–	[22]
WS_2	1558.5, 1566	7.5	8.83	0.6	10.1	1.14	[38]
WS_2	1531.5, 1557.5	0.42	2.14	11	14.2	6.64	In this work

the pump power reaches to 420 mW, the maximum output power of the dual-wavelength soliton laser is about 14.2 mW, which is higher than the previous reports [32–39]. This may be relates to the lower nonsaturated loss and smaller insert loss of as-used WS_2 device. In addition, Table 1 summaries the dual-wavelength soliton lasers near 1550 nm. Clearly, similar to the other nanomaterials (CNTs, Bi_2Te_3, and h-BN), few-layer WS_2 also exhibits excellent nonlinear optical properties.

Slightly tuning the PC, the other soliton state also can be obtained in the fiber laser. Fig. 5 shows the typical noise-like pulse operation at a pump power of 300 mW. The output spectrum exhibits a triangular profile with the bandwidth of 0.48 nm, as shown in Fig. 5(a). The temporal profile is illustrated in Fig. 5(b), in which the interval between adjacent pulses is equal to the cavity round trip (467.4 ns). As shown in the inset of Fig. 5(b), the pulse pocket consists of multiple incoherent pulses with randomly distributed intensities and phases, which may be caused by the Raman effect in the laser cavity [48]. Meanwhile, it follows the Gauss fitting well. When the pump power is 300 mW, the output power of laser is about 10.2 mW, corresponding to the pulse energy of 4.74 nJ. Clearly, the pulse energy is larger than that of the conventional soliton (~0.1 nJ), which accords with the high-energy characteristics of noise-like pulse [4,20].

In the above experiment, it is difficult to obtain conventional soliton output whatever adjusting the cavity parameters, such as the pump strength and polarization states. According to the soliton theory [47], the formation of conventional soliton is caused by the balance between the cavity dispersion and self-phase modulation in the cavity. To this end, we will optimize the cavity dispersion by increasing or decreasing the length of SMF in our proposed laser cavity. With this approach, we indeed obtained the conventional soliton under different cavity dispersions. For example, the stable conventional soliton and its harmonic form can be obtained with a length of SMF of ~90 m, which corresponds to the cavity dispersion parameter value of -2 ps^2. By properly rotating the PC and adjusting the pump power, we obtained the conventional soliton pulse at the pump power of 180 mW in our proposed fiber laser. Its optical spectrum is shown in Fig. 6(a). The 3-dB spectral bandwidth is about 0.32 nm. Correspondingly, a typical pulse train, depicted in Fig. 6(b), has a period of 271.2 ns, which matches with the cavity roundtrip time, verifying the mode-locking operation of the fiber laser. In addition, we also provided its autocorrelation trace, as illustrated in the inset of Fig. 6(b). If a sech^2 profile is assumed for fitting, the pulse duration is about 7.8 ps. Thus, the TBP is ~0.32, which indicates that the soliton pulse was nearly chirped-free. In order to examine the long-term stability of the soliton pulses, we continuously monitor their output spectra for 7 h, as shown in Fig. 6(c).

Harmonic mode-locking (HML) is one of the intrinsic characteristics of soliton operation in passively mode-locked fiber lasers. Fig. 7(a) shows the optical spectrum of HML pulse. It can be seen that, the Kelly sidebands on the spectrum disappear, implying the HML state generation dissatisfies the phase-matching condition for the formation of the Kelly sidebands [47]. The pulse train is shown in Fig. 7(b). The time

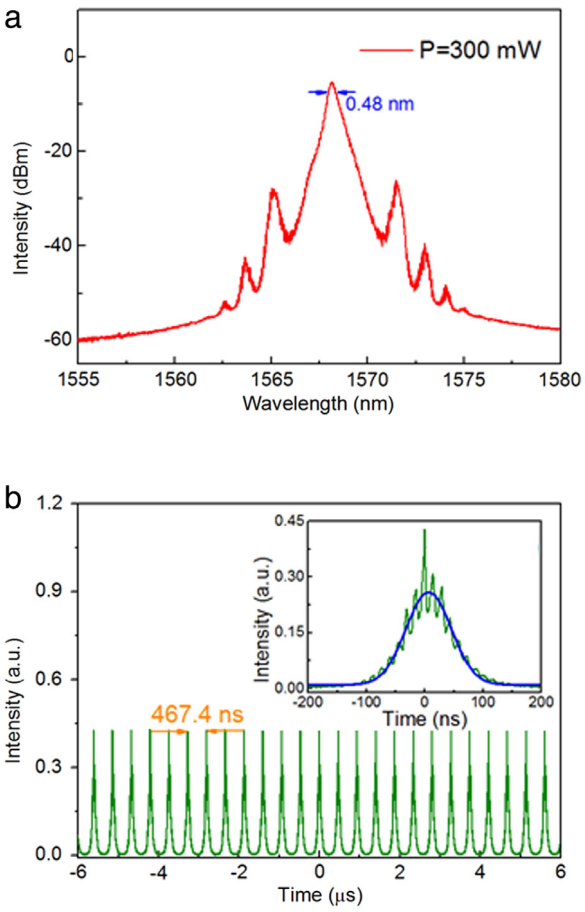

Fig. 5. (a) Optical spectrum and (b) pulse train of noise-like pulse, inset: zoom-in image of single pulse and its Gauss fitting (blue solid line). (For interpretation of the references to colour in this figure legend, the reader is referred to the web version of this article.)

interval of the pulse train is about 2.01 ns, corresponding to a repetition rate of ~497.5 MHz, which is the 135th harmonics of the fundamental repetition rate (3.69 MHz). It is the highest harmonic number in the WS_2 mode-locked fiber lasers, to the best of our knowledge. Furthermore, we also provide the relation between harmonic numbers versus pump power, as shown in Fig. 7(c). On the whole, the harmonic number increases almost linearly with the pump power. Also, when the laser reaches to its maximum pump power of 420 mW, we can obtain different harmonic numbers, which may be caused by the polarization-dependent loss under different polarization states. Notably, the pulse repetition rate could be further increased with the higher pump power.

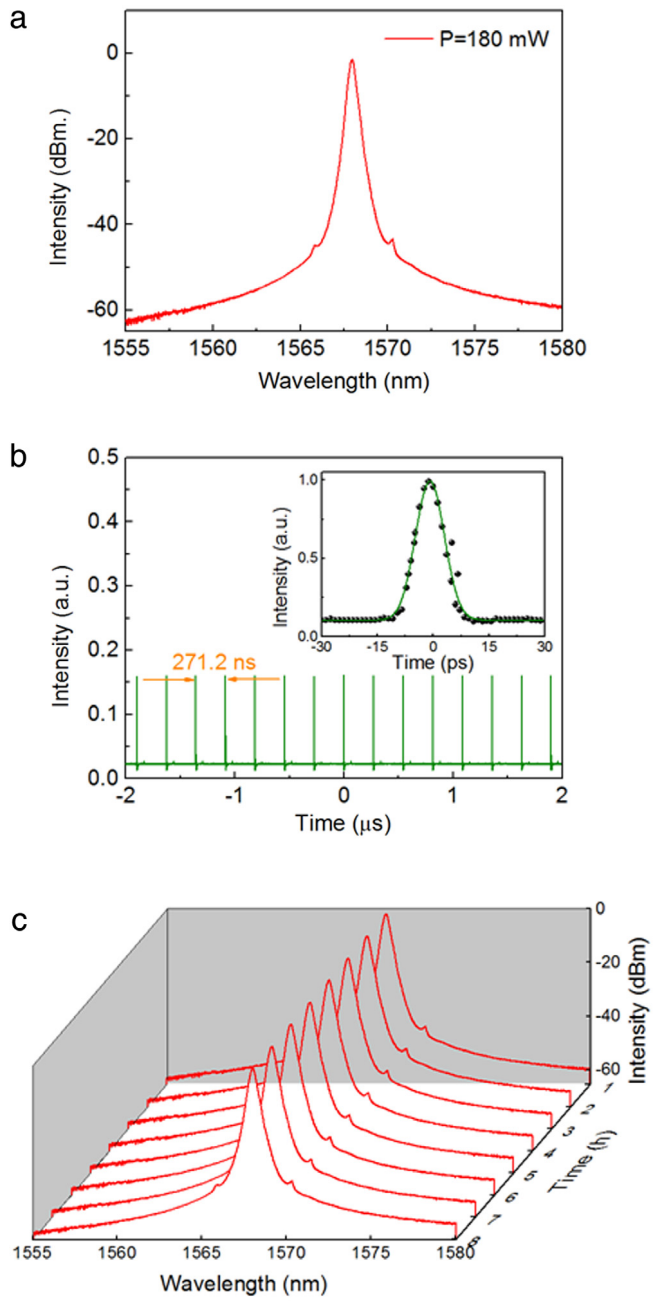

Fig. 6. Conventional soliton operation with the SMF length of ~90 m: (a) optical spectrum, (b) its corresponding oscilloscope trace (inset: the autocorrelation trace), (c) long-term optical spectra measured at a 1-h interval over 7 h.

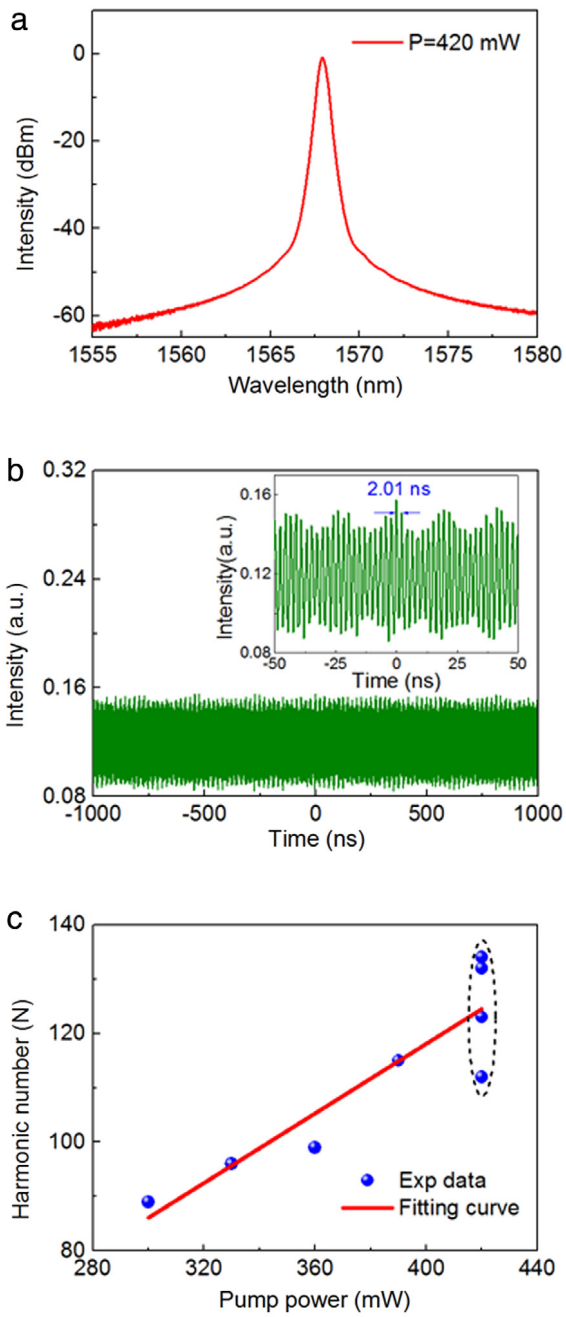

Fig. 7. HML performance of conventional soliton pulse: (a) Spectrum; (b) pulse train (Inset: the pulse distribution in full range with 100 ns; (c) harmonic number versus pump power. In the short-line circle, the harmonic number varies different polarization states.

The formation of the versatile soliton pulses in our laser cavity can be explained as follows. Besides saturable absorption ability, the few-layer WS_2 itself shows a high nonlinear effect. Furthermore, we fabricated a microfiber and optically deposited the few-layer WS_2 onto it, the evanescent field interaction of few-layer WS_2 and microfiber will also greatly enhance the cavity nonlinearity. Thus, taking into account these two contributions, a single soliton circulating in the cavity can be split into multiple soliton pulses under high pump power. In such regime, these pulses are usually randomly located in the cavity. However, they can automatically arrange themselves in the laser cavity forming the dual-wavelength soliton and HML state by properly adjusting the polarization state. Otherwise, the noise-like pulse can be generated under proper cavity parameters.

Finally, it can be expected that other soliton pulse patterns, such as dissipative soliton resonance [22], and multiple soliton molecules [26] could be also observed by using a WS_2 photonic device in the laser cavity in future work. In addition, other 2D materials, such as TIs [21–23] and BPs [30], have also been demonstrated to possess huge nonlinear refractive indexes. Thus, other 2D materials-based devices can also be used to explore the versatile soliton pulses in the fiber lasers in future work.

5. Conclusion

We have experimentally achieved the versatile soliton pulses from a passively mode-locked fiber laser incorporating with a microfiber-based WS_2 device. The WS_2-deposited microfiber could both operate

as a mode-locker for soliton generation and a high-nonlinear device for versatile soliton generation. By utilizing the saturable absorption and high-nonlinear effect of the WS_2 device, conventional soliton and its harmonic form, dual-wavelength soliton, and noise-like soliton pulse have been achieved by properly adjusting the pump strength and the polarization state in the laser cavity. For the dual-wavelength soliton pulses and noise-like pulse, the output power of 14.2 mW and pulse energy of 4.74 nJ is obtained, respectively. In addition, we also achieve the harmonic number (135) of conventional soliton, **c**orresponding to a repetition rate of ~497.5 MHz. Our study indicates that the microfiber-based WS_2 device could be as an excellent dual-function device for studying a great deal of nonlinear phenomena.

Acknowledgments

This work was supported by the Program for equipment pre-research field funds under grant 6140414040116CB01012 and the Fundamental Research Funds for the Central Universities (GK2110260153), National Natural Science Foundation (61575050 and 61575051), Key Program for International S&T Cooperation Projects of China under grant 2016YFE0126500, Key Program for Natural Science Foundation of Heilongjiang Province of China under grant ZD2016012, and the 111 project of the Harbin Engineering University (B13015).

References

[1] U. Keller, Nature 424 (2003) 831.
[2] B. Oktem, C. Ülgüdür, F. Ö Ilday, Nat. Photonics 4 (2010) 307.
[3] P. Grelu, N. Akhmediev, Nat. Photonics 6 (2012) 84.
[4] M. Horowitz, Y. Barad, Y. Silberberg, Opt. Lett. 22 (1997) 799.
[5] M.K. Islam, T.O. Tsun, P.L. Chu, OSA Trends Opt. Photonic Ser. (TOPS) 16 (1997) 181.
[6] W.C. Chen, Z.C. Luo, W.C. Xu, Laser Phys. Lett. 6 (2009) 816.
[7] D. Mao, H. Lu, J. Opt. Soc. Amer. B 29 (2012) 2819.
[8] Z.C. Luo, A.P. Luo, W.C. Xu, J.R. Liu, H.S. Yin, Appl. Phys. B: Lasers Opt. 100 (2010) 811–820.
[9] D. Mao, X.M. Liu, L.R. Wang, X.H. Li, H. Lu, H.B. Sun, Y.K. Gong, Laser Phys. 20 (2010) 847.
[10] L. Yun, D. Han, Opt. Commun. 285 (2012) 5406.
[11] X. Zhao, Z. Zheng, L. Liu, Y. Liu, Y. Jiang, X. Yang, J. Zhu, Opt. Express 19 (2011) 1168.
[12] G.W. Chen, W.L. Li, H.R. Yang, Y.C. Kong, J. Modern Opt. 62 (2015) 353–357.
[13] C. Zeng, Y.D. Cui, J. Guo, Opt. Commun. 347 (2015) 44.
[14] B. Guo, S. Li, K. Zhang, Y. Fan, Z. Fang, J. Ren, L. Yuan, P. Wang, ChinaXiv preprint www.chinaxiv.org/abs/201611.00719.
[15] L.A. Vazquez-Zuniga, Y. Jeong, IEEE Photonics Technol. Lett. 24 (2012) 1549.
[16] Q. Bao, H. Zhang, Y. Wang, Z. Ni, Y. Yan, Z.X. Shen, K.P. Loh, D.Y. Tang, Adv. Funct. Mater. 19 (2009) 3077.
[17] A. Martinez, Z. Sun, Nat. Photonics 7 (2013) 842.
[18] Y. Meng, S. Zhang, X. Li, H. Li, J. Du, Y. Hao, Opt. Express 20 (2012) 6685.
[19] X. Li, K. Wu, Z. Sun, B. Meng, Y. Wang, Y. Wang, X. Yu, Y. Zhang, P. Shum, Q.J. Wang, Sci. Rep. 6 (2016) 25266.
[20] G. Sobon, J. Sotor, A. Przewolka, I. Pasternak, W. Strupinski, K. Abramski, Opt. Express 24 (2016) 20359.
[21] C. Zhao, H. Zhang, X. Qi, Y. Chen, Z. Wang, S. Wen, D. Tang, Appl. Phys. Lett. 101 (2012) 211106.
[22] M. Liu, N. Zhao, H. Liu, X.W. Zheng, A.P. Luo, Z.C. Luo, W.C. Xu, C.J. Zhao, H. Zhang, S.C. Wen, IEEE Photonics Technol. Lett. 26 (2014) 983–986.
[23] B. Guo, Y. Yao, J. Xiao, R.L. Wang, J.Y. Zhang, IEEE J. Sel. Top. Quantum Electron. 22 (2016) 1–8.
[24] K. Wang, J. Wang, J. Fan, M. Lotya, A. O'Neill, D. Fox, Y. Feng, X. Zhang, B. Jiang, Q. Zhao, H. Zhang, J.N. Coleman, L. Zhang, W.J. Blau, ACS Nano 7 (2013) 9260.
[25] H. Zhang, S.B. Lu, J. Zheng, J. Du, S.C. Wen, D.Y. Tang, K.P. Loh, Opt. Express 22 (2014) 7249.
[26] A.P. Luo, M. Liu, X.D. Wang, Q.Y. Ning, W.C. Xu, Z.C. Luo, Photon. Res. 3 (2015) A69.
[27] Z. Luo, Y. Li, M. Zhong, Y. Huang, X. Wan, J. Peng, J. Weng, Photon. Res. 3 (2015) A79.
[28] S. Yu, X. Wu, Y. Wang, X. Guo, L. Tong, Adv. Mater. 7 (2017) 1606128.
[29] Y. Chen, G. Jiang, S. Chen, Z. Guo, X. Yu, C. Zhao, H. Zhang, Q. Bao, S.C. Wen, D. Tang, D. Fan, Opt. Express 23 (2015) 12823.
[30] X. Wang, S. Lan, Adv. Opt. Photon. 8 (2016) 618.
[31] D. Mao, Y. Wang, C. Ma, L. Han, B. Jiang, X. Gan, S. Hua, W. Zhang, T. Mei, J. Zhao, Sci. Rep. 5 (2015) 7965.
[32] P. Yan, A. Liu, Y. Chen, H. Chen, S. Ruan, C. Guo, S. Chen, L. Li, H. Yang, J. Hu, G. Cao, Opt. Mater. Express 5 (2015) 479.
[33] M. Jung, J. Lee, J. Park, J. Koo, Y.M. Jhon, J.H. Lee, Opt. Express 23 (2015) 19996.
[34] R. Khazaeinezhad, S.H. Kassani, H. Jeong, K.J. Park, B.Y. Kim, D.I. Yeom, K. Oh, IEEE Photonics Technol. Lett. 27 (2015) 1581.
[35] L. Li, S. Jiang, Y. Wang, X. Wang, L. Duan, D. Mao, Z. Li, B. Man, J. Si, Opt. Express 23 (2015) 28698.
[36] J. Hou, G. Zhao, Y. Wu, J. He, X. Hao, Opt. Express 23 (2015) 27292.
[37] P. Yan, A. Liu, Y. Chen, J. Wang, S. Ruan, H. Chen, J. Ding, Sci. Rep. 5 (2015) 12587.
[38] B. Guo, Y. Yao, P.G. Yan, K. Xu, J.J. Liu, S.G. Wang, Y. Li, IEEE Photonics Technol. Lett. 28 (2016) 323.
[39] W. Liu, L. Pang, H. Han, M. Liu, M. Lei, S. Fang, H. Teng, Z. Wei, Opt. Express 25 (2017) 2950.
[40] K. Wu, X. Zhang, J. Wang, X. Li, J. Chen, Opt. Express 23 (2014) 11453.
[41] B. Chen, X. Zhang, K. Wu, H. Wang, J. Wang, J. Chen, Opt. Express 23 (2015) 26723.
[42] M. Zhang, G. Hu, R.C.T. Howe, L. Chen, Z. Zheng, T. Hasan, 2015. arXiv preprint arXiv:1507.03188.
[43] J. Lin, K. Yan, Y. Zhou, L.X. Xu, C. Gu, Q.W. Zhan, Appl. Phys. Lett. 107 (2015) 191108.
[44] Z. Luo, D. Wu, B. Xu, H. Xu, Z. Cai, J. Peng, J. Weng, S. Xu, C. Zhu, F. Wang, Z. Sun, H. Zhang, Nanoscale 8 (2016) 1066.
[45] C. Luan, K. Yang, J. Zhao, S. Zhao, L. Song, T. Li, H. Chu, J. Qiao, C. Wang, Z. Li, S. Jiang, B. Man, L. Zheng, Opt. Lett. 41 (2016) 3783.
[46] S. Huang, Y. Wang, P. Yan, J. Zhao, H. Li, R. Lin, Opt. Express 22 (2014) 11417.
[47] G.P. Agrawal, Nonlinear Fiber Optics, fifth ed., Academic, San Francisco, CA, USA, 2013.
[48] J. Xu, S. Wu, J. Liu, J. Ren, T. Yang, Q. Yang, P. Wang, Chin. J. Lasers 41 (2014) 29.